Generalized phase mixing: Turbulence-like behaviour from unidirectionally propagating MHD waves

Norbert Magyar,* Tom Van Doorsselaere, and Marcel Goossens
Centre for mathematical Plasma Astrophysics (CmPA),
KU Leuven, Celestijnenlaan 200B bus 2400, 3001 Leuven, Belgium;
(Dated: February 9, 2017)

We present the results of three-dimensional (3D) ideal magnetohydrodynamics (MHD) simulations on the dynamics of a perpendicularly inhomogeneous plasma disturbed by propagating Alfvénic waves. Simpler versions of this scenario have been extensively studied as the phenomenon of phase mixing. We show that, by generalizing the textbook version of phase mixing, interesting phenomena are obtained, such as turbulence-like behavior and complex current-sheet structure, a novelty in longitudinally homogeneous plasma excited by unidirectionally propagating waves. This constitutes an important finding for turbulence-related phenomena in astrophysics in general, relaxing the conditions that have to be fulfilled in order to generate turbulent behavior.

arXiv:1702.02346v1 [astro-ph.SR] 8 Feb 2017

Phase mixing of Alfvén waves, in the context of astrophysics, was originally suggested as a candidate mechanism to heat both the open magnetic field corona (e.g. coronal holes) and coronal loops[1]. Heating is achieved through small scale generation: Alfvén waves excited in the lower solar atmosphere propagate outward, and neighbouring oscillating field lines get out of phase if a varying Alfvén speed profile is present transverse to the propagation direction. Once the resulting scales are small enough, viscous and/or resistive dissipation occurs. Another, increasingly popular wave heating (AC) mechanism (it can also be viewed as a DC mechanism in case of quasi-static driving[2]) proposed for heating the solar corona[3] is MHD turbulence[4–8], which has general applications in astrophysics[9, 10], as well as in the physics of fusion and numerous industrial applications[11, 12]. The underlying idea for energy conversion is the same as in phase mixing: small scales are generated by the nonlinear cascade of wave energy, until the dissipation range is reached. For turbulence to be sustained in incompressible MHD, counterpropagating waves need to be present in the medium [13]. One often uses the Elsässer variables ($\mathbf{z}^{\pm} = \mathbf{v} \pm \mathbf{b}/\sqrt{4\pi\rho}$, where $\mathbf{v}$ is velocity, $\mathbf{b}$ is magnetic field and ρ is plasma density) to better differentiate between outward ($-$) and inward ($+$) propagating Alfvén waves, for an outwardly directed mean magnetic field $\mathbf{B}_0$[9, 14, 15]. Note that this holds only in incompressible MHD. In plasma with a finite speed of sound, compressible modes, i.e. fast and slow MHD waves are present. However, in a general inhomogeneous plasma, the MHD waves have mixed properties and cannot be decoupled [16]. In this case, by using compressible Elsässer variables (same as above but with varying density, see [17]) we can still keep the Elsässer formalism, but generally we can no longer interpret the variables as representing parallel and anti-parallel propagating Alfvén waves, due to contributions from the compressible modes. In the incompressible case, starting from a spectrum of purely outgoing Alfvén waves (e.g. as in a coronal hole), a source of incoming waves is necessary for nonlinear interactions to sustain MHD turbulence. This source can be the inhomogeneities, so-called large-scale gradients in the plasma (e.g. gravitational stratification in a coronal hole), causing reflections of the waves[2, 18–20]. However, if we consider compressible modes, nonlinear interactions ($\mathbf{z}^{\pm} \neq 0$) are no longer restricted to counterpropagating Alfvén waves: in an inhomogeneous medium, propagating MHD waves have mixed properties, and appear differently (predominantly Alfvén or fast characteristics) in different regions of the plasma, dictated by the local inhomogeneity [21]. This can be viewed, in the Elsässer formalism, as waves presenting both $\mathbf{z}^{+}$ and $\mathbf{z}^{-}$ fields to a varying degree, depending on the local inhomogeneity. In this sense, nonlinear terms represent self-deformation of waves [17].

We employ 3D ideal MHD numerical simulations to test this scenario, using `MPI-AMRVAC`[22, 23]. Our numerical domain is $1 \times 1 \times 20$ Mm in size, discretized with $512 \times 512 \times 128$ numerical cells, representing a thin elongated section of a coronal hole. We consider a straight, homogeneous magnetic field of 5 G directed along the z-axis. Gravity is neglected, thus there is no stratification along the magnetic field. The plasma $\beta \approx 0.15$ is constant throughout the domain at $t = 0$. The large-scale gradient transverse to the magnetic field is given by inserting, on a uniform background density of $2 \cdot 10^{-13}$ kg m^{-3}, 250 random (in position and width) Gaussian density enhancements in the $x - y$ plane, uniform along the z-axis, aiming to represent random perpendicular density variations in a coronal hole, in equilibrium. The structure is periodic in the $x - y$ plane, as we set periodic boundaries laterally. The resulting mean density is $\approx 1.2 \cdot 10^{-12}$ kg m^{-3}, while the peak is $\approx 3 \cdot 10^{-12}$ kg m^{-3} . At the top boundary, we use a Neumann-type zero-gradient 'open' boundary condition for all variables. At the bottom, we employ a wave driver with properties intending to mimic observed Alfvénic waves in coronal holes[20, 24]. In this sense, we use a superposition of 10 sinusoidal waves, each with a definite period, amplitude (obtained randomly from the observed

log-normal distributions[20]), and random direction. The driver is time but not space-dependent, i.e. the whole boundary is driven equally. The resulting rms velocity amplitude is $\approx$ 12 km s^{-1}. This magnitude shows us that we are in the weakly compressible, subsonic regime of flow ($\mathbf{v}_{rms} < V_A$).

We run the simulation for 1000 s. During this time, perturbations originating from the boundary driver propagate upwards (on the z-axis) and interact with the inhomogeneities. The initial (equilibrium) transverse structure is quickly destroyed by the propagating Alfvénic waves, and transformed into a cross-section presenting structures on a large range of scales, reminiscent of turbulence (see FIG. 1). This observation was at the basis of a previous study which doubts the existence of packed thin individual and dynamically independent magnetic elements in the solar corona, so-called 'coronal strands' or filaments, when perturbed by propagating Alfvénic waves[25]. The current density shows the same turbulence-like structure in the cross-section with numerous current sheets forming (see FIG.2) and getting dissipated by numerical resistivity. Note how the current in individual strong current sheets is more than an order of magnitude stronger than the average current density. The peak values in the current density depend on the resolution and numerical resistivity, but should ultimately saturate at sufficiently high resolutions. In test runs with half resolution, the peak values drop approximately to half as compared to FIG. **??**, indicating that we did not reach the saturated state. The dissipation (heating) leads to an increase in the internal energy of the plasma. However, this represents only a $\approx 2.2\%$ rise with respect to the equilibrium value of the internal energy, being unable to change the plasma temperature significantly. Heat sources or sinks, thermal conduction or thin radiative losses are not included in the energy equation.

We calculated the 1D power spectra of magnetic and kinetic energy, density, pressure (shown in FIG 3), and $\mathbf{z}^{\pm}$ (not shown, for clarity) in a plane perpendicular to the mean magnetic field $\mathbf{B}_0$. Note that the small scale generation or cascade is purely perpendicular to the mean magnetic field $\mathbf{B}_0$. We use the `fft` routine of `IDL` to obtain $|\mathbf{f}_{k_x,k_y}|^2$, where $\mathrm{f} = \mathbf{v}, \mathbf{b}, \mathbf{z}^{\pm}, \rho, \mathrm{p}$. The magnetic and kinetic energy spectrum is then

$$E_{KM}(k_\perp) = \sum_{k_x,k_y} \left(|\mathbf{v}_{k_x,k_y}|^2 + |\mathbf{b}_{k_x,k_y}|^2\right),\ k_\perp = \sqrt{k_x^2 + k_y^2} \tag{1}$$

while the calculation is similar for the other variables. Note, however, that E_{KM} is not the total energy: in compressible MHD the total energy contains also the internal energy [17]. We chose to calculate their spectra separately as the contribution from the internal energy is an order of magnitude higher than E_{KM}. The time-averaged energy spectrum ($k_\perp^{-2.54}$) is steeper than the well-known MHD inertial range spectra of $k_\perp^{-5/3}$. However, we did not expect to recover the (strong) MHD turbulence spectra since our dynamics resembles an unsteady, unbalanced weak MHD turbulence, with tempo-spatial varying energy ratio of the $\mathbf{z}^{\pm}$ fields. Currently, there are no analytical or even phenomenological models describing this scenario in compressible MHD. No attempt is made here to develop such a model. The closest incompressible MHD turbulence description to the present scenario is that of unbalanced weak MHD turbulence [26]. Note, however, that there are still fundamental differences with respect to the incompressible case: The nonlinear cascade in our system is not driven by counterpropagating Alfvén waves as in the latter, but by the mixed properties of MHD waves in an inhomogeneous plasma, presenting self-deformation. The inertial range spectra changes in time due to the varying boundary driver, and the varying generation of the secondary component of $\mathbf{z}^+$ (see FIG. 4), thus the aforementioned varying E^-/E^+ ($E^{\pm} = |\mathbf{z}^{\pm}(k_\perp)|^2$) Elsässer energy ratio. In FIG. 3 we also show the energy spectrum at $t = 500$ s, which presents an inertial range slope close to that in weak MHD turbulence[9, 27], k^{-2}. In unbalanced weak MHD turbulence, $E^{\pm} \propto k_\perp^{-2\pm\alpha}$[28], where $\alpha \neq 0$ and corresponds to different inertial range slopes for Elsässer energies. We get $\approx\ -1.85$ and -2.01 for the E^+ and E^- inertial range slopes, respectively, at $t = 500$ **s**. The time-average slopes are $\approx\ -2.08$ and -2.8, respectively. The pinning effect (converging $E^{\pm}$ spectra at the dissipation range, see [26]) of the Elsässer energies is observed, around $k_\perp = 0.02$ km^{-1}. There is a striking difference in the inertial range slopes of pressure and density: for a polytropic law, dimensional analysis leads us to similar $k^{-7/3}$ slopes for both variables, which should be valid even in weakly compressible cases, as the present one [9]. The deviation from this law might come from the use of a full energy equation instead of a polytopic relation, which allows us to set up a moderately inhomogeneous density profile while setting the pressure constant initially. In FIG. 4 the $\mathbf{z}^+$ field is shown, as well as the $\mathbf{z}^-$ contours. Note that these two fields do not represent two different waves: they are the manifestations of MHD waves with mixed properties. The dominant component of the waves is the $\mathbf{z}^-$ field, showing that the driven wave has a largely Alfvénic character [29]. We can see that the $\mathbf{z}^{\pm}$ propagation directions coincide, and there appears to be no significant reflection (tests with homogeneous density runs show maximum 0.5% reflection of the incident wave energy) on the top boundary (at $z = 20$ Mm). Also, $|\mathbf{z}^+|$ displays a bursty, patchy evolution, as expected from the high degree of perpendicular density inhomogeneity in the domain. This might explain the observed rapid variation of the calculated spectra. To further strengthen our point about the origin of the $|\mathbf{z}^+|$ field, we ran additional simulations, identical to the presented one, except removing the inhomogeneities in density for $z \geq 10$ Mm, i.e. a

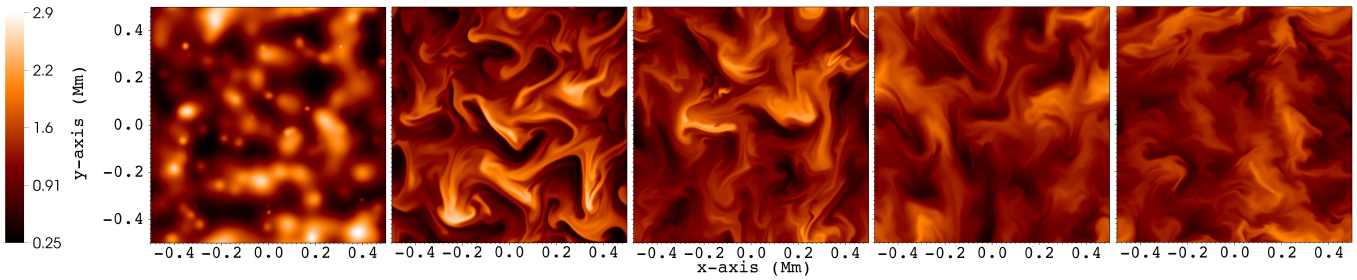

FIG. 1. Evolution of density in a 2D slice taken at *zaverage* = 18 Mm, shown in steps of 250 s (to the right), the first plot showing the equilibrium transverse structure ($t = 0$ s). The density color legend is shown in units of 10^{-12} kg m^{-3}.

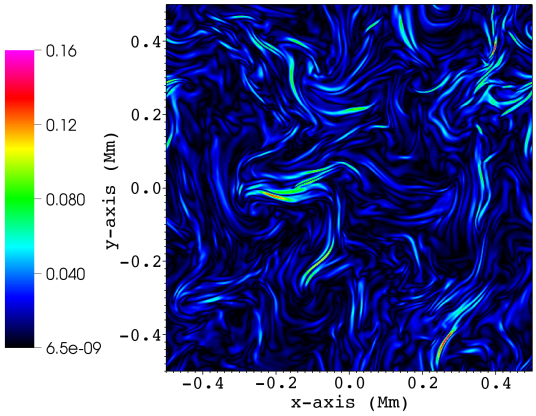

FIG. 2. Absolute value of current density (user units) along the z-axis (j_z) in a 2D slice taken at $z = 18$ Mm and $t = 500$ s.

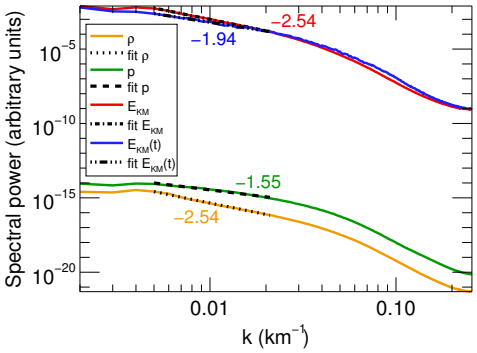

FIG. 3. Spectra (power spectral density) of energy ('E_{KM}' - time averaged over $200 - 1000$ s; 'E_{KM}(t)' - energy spectrum at $t = 500$ s), density, and pressure ('ρ, p' - time averaged over $200 - 1000$ s) calculated in a perpendicular slice at $z = 18$ Mm. Linear fits to the inertial range are also shown for each spectrum. Values for the slopes are also shown, in matching colors.

sudden transition to the constant background density. In FIG. 5, the resulting $\mathbf{z}^{\pm}$ fields are shown at $t = 30$ s, i.e. just before the first wavefront reaches the top z boundary. We chose this early snapshot in order to partially exclude the waves reflected at $z = 10$ Mm, which otherwise would dominate the $|\mathbf{z}^+|$ field and hide the $|\mathbf{z}^+|$ contribution resulting from the mixed properties of the waves. The reflected waves are counter-propagating[2], and can be seen in FIG. 5 as the strong wavefronts originating from $z = 10$ Mm. Note how the $|\mathbf{z}^+|$ component is practically absent in the homogeneous region $z \geq 10$ Mm, but there's an even stronger $|\mathbf{z}^-|$, as a consequence of conservation of energy. In this sense, the $|\mathbf{z}^+|$ in the inhomoegeneous region (excluding the contribution from the reflected counter-propagating waves) is a manifestation of a unidirectionally propagating wave with mixed properties in a perpendicularly inhomogeneous medium and cannot be associated with a different wave.

We performed a first, full 3D MHD simulation of a generalized phase mixing scenario, with the varying Alfvén speed in the domain given by a random density profile perpendicular to the mean magnetic field. The equilibrium is perturbed by upward-travelling Alfvénic waves, modeled after the observed properties of waves

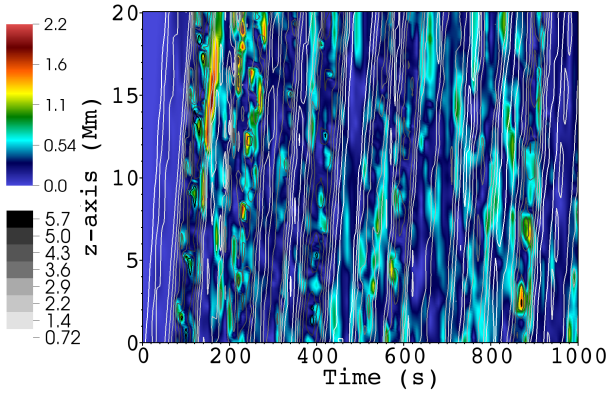

FIG. 4. Time-distance map of $|\mathbf{z}^-|$ (greyscale contour plot) and $|\mathbf{z}^+|$ (color plot) along the segment $(x, y, z) = (0, 0, z)$. The step-like appearance of some wave-fronts is a visualization artifact, due to limited number of snapshots in time (100). Values are in user units.

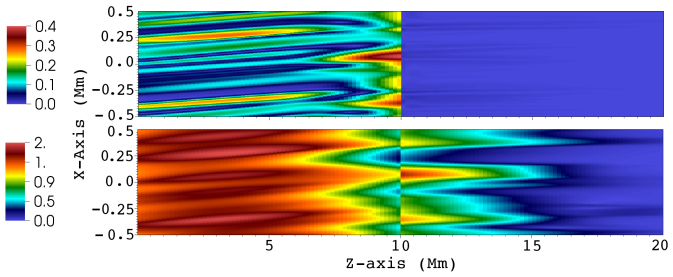

FIG. 5. Snapshots of $|\mathbf{z}^+|$ (top) and $|\mathbf{z}^-|$ (bottom) in the $(x, 0, z)$ plane at $t = 30$ s, of the setup with homogeneous background density after $z \geq 10$ Mm, with corresponding color legends on the sides. Values are in user units.

in coronal holes. The resulting dynamics are complex and turbulence-like in the cross-section, however the solution remains smooth parallel to the z-axis. Current sheets form in the process, displaying ribbon-like appearance along the main magnetic field, when viewed in 3D. These current sheets are dissipated and this leads to a small rise in the internal energy. This heating (at least in this setup) does not cause significant changes to the average temperature in the domain. The driven propagating wave has mixed properties due to the inhomogeneities, manifesting as simultaneous nonzero $\mathbf{z}^{\pm}$ fields, presenting nonlinear self-deformation, in this sense. The perpendicular spectrum of energy displays a power-law like appearance. This spectrum is highly variable in time, and its average slope for the inertial range is not in accordance with any presently available theory, being steeper than the $k_{\perp}^{-2}$ law in weak MHD turbulence. However, there is a clear separation of inertial and dissipation ranges, and the pinning effect, observed in numerical simulations of unbalanced weak MHD turbulence, is present. These findings might relax the criteria for the existence of turbulence-like cascade in plasma with a mean magnetic field and large-scale inhomogeneities perpendicularly to it. As this scenario is likely frequently present in astrophysical context, it might make turbulence-like behavior nearly ubiquitous. This might be relevant also in other fields dealing with turbulence, such as in fusion and industrial applications.

N.M. thanks Francesco Pucci and Vyacheslav Olshevskyi for fruitful discussions. N.M. acknowledges the Fund for Scientific Research-Flanders (FWO-VLaanderen). T.V.D. was supported by an Odysseus grant. T.V.D. and M.G. acknowledges support by the Belspo IAP P7/08 CHARM network and the GOA-2015-014 (KU Leuven).

* norbert.magyar@kuleuven.be; FWO (Fonds Wetenschappelijk Onderzoek) PhD fellow.

[1] J. Heyvaerts and E. R. Priest, A&A **117**, 220 (1983).
[2] W. H. Matthaeus, D. J. Mullan, P. Dmitruk, L. Milano, and S. Oughton, Nonlinear Processes in Geophysics **10**, 93 (2003).
[3] I. Arregui, Philosophical Transactions of the Royal Society of London Series A **373**, 20140261 (2015), arXiv:1501.06708 [astro-ph.SR].
[4] G. Einaudi, M. Velli, H. Politano, and A. Pouquet, ApJ **457**, L113 (1996).
[5] P. Dmitruk, W. H. Matthaeus, L. J. Milano, S. Oughton, G. P. Zank, and D. J. Mullan, Astrophys. J. **575**, 571 (2002), astro-ph/0204347.
[6] A. F. Rappazzo, M. Velli, G. Einaudi, and R. B. Dahlburg, Astrophys. J. **677**, 1348-1366 (2008), arXiv:0709.3687.
[7] A. A. van Ballegooijen, M. Asgari-Targhi, S. R. Cranmer, and E. E. DeLuca, Astrophys. J. **736**, 3 (2011), arXiv:1105.0402 [astro-ph.SR].
[8] A. A. van Ballegooijen, M. Asgari-Targhi, and M. A. Berger, Astrophys. J. **787**, 87 (2014).
[9] D. Biskamp, *Magnetohydrodynamic Turbulence, by Dieter Biskamp, pp. 310. ISBN 0521810116. Cambridge, UK: Cambridge University Press, September 2003.* (2003) p. 310.
[10] A. Beresnyak and A. Lazarian, in *Magnetic Fields in Diffuse Media*, Astrophysics and Space Science Library, Vol. 407, edited by A. Lazarian, E. M. de Gouveia Dal Pino, and C. Melioli (2015) p. 163, arXiv:1406.1185.
[11] K. S. Reddy and M. K. Verma, Physics of Fluids **26**, 025109 (2014).
[12] P. Manas, W. A. Hornsby, C. Angioni, Y. Camenen, and A. G. Peeters, Plasma Physics and Controlled Fusion **59**, 035002 (2017).
[13] P. Dmitruk, W. H. Matthaeus, L. J. Milano, and S. Oughton, Physics of Plasmas **8**, 2377 (2001).
[14] W. M. Elsasser, Physical Review **79**, 183 (1950).
[15] M. Dobrowolny, A. Mangeney, and P. Veltri, A&A **83**, 26 (1980).
[16] A. De Groof and M. Goossens, A&A **356**, 724 (2000).
[17] E. Marsch and A. Mangeney, J. Geophys. Res. **92**, 7363 (1987).
[18] M. Velli, R. Grappin, and A. Mangeney, Physical Review Letters **63**, 1807 (1989).
[19] W. H. Matthaeus, G. P. Zank, S. Oughton, D. J. Mullan, and P. Dmitruk, ApJ **523**, L93 (1999).
[20] R. J. Morton, S. Tomczyk, and R. Pinto, Nature Communications **6**, 7813 (2015).
[21] I. Arregui and et al., in preparation (2017).
[22] R. Keppens, Z. Meliani, A. J. van Marle, P. Delmont, A. Vlasis, and B. van der Holst, Journal of Computational Physics **231**, 718 (2012).
[23] O. Porth, C. Xia, T. Hendrix, S. P. Moschou, and R. Keppens, ApJS **214**, 4 (2014), arXiv:1407.2052 [astro-ph.IM].
[24] S. W. McIntosh, B. de Pontieu, M. Carlsson, V. Hansteen, P. Boerner, and M. Goossens, Nature (London) **475**, 477 (2011).
[25] N. Magyar and T. Van Doorsselaere, Astrophys. J. **823**, 82 (2016), arXiv:1604.04078 [astro-ph.SR].
[26] S. Boldyrev and J. C. Perez, Physical Review Letters **103**, 225001 (2009), arXiv:0907.4475 [astro-ph.GA].
[27] C. S. Ng and A. Bhattacharjee, Physics of Plasmas **4**, 605 (1997).
[28] S. Galtier, S. V. Nazarenko, A. C. Newell, and A. Pou-

quet, Journal of Plasma Physics **63**, 447 (2000), astro-ph/0008148.

[29] M. Goossens, R. Soler, J. Terradas, T. Van Doorsselaere, and G. Verth, Astrophys. J. **788**, 9 (2014).